

# Spatial and Energetic Stability Assessment of the Adducts of Phytocompounds of *Piper longum* L. with $\alpha$ -amylase by Computational Approach

Sujan Dhital<sup>1</sup>, Nirmal Parajuli<sup>1</sup>, Manila Poudel<sup>2</sup>, Timila Shrestha<sup>1</sup>, Samjhana Bharati<sup>1</sup>,

Binita Maharjan<sup>1</sup>, Bishnu Prasad Marasini<sup>3</sup>, Jhashanath Adhikari Subin<sup>4,\*</sup> ,

Ram Lal Swagat Shrestha<sup>1,\*</sup> 

<sup>1</sup> Department of Chemistry, Amrit Campus, Tribhuvan University, Lainchaur, Kathmandu 44600, Nepal; sujandhital07@gmail.com (S.D.); parajulinirmal1999@gmail.com (N.P.); timilastha@gmail.com (T.S.); bharati.samjhana@gmail.com (S.B.); binitamhrjan@gmail.com (B.M.); swagatstha@gmail.com (R.L.S.S.);

<sup>2</sup> Department of Biotechnology, National College, Tribhuvan University, Lainchaur, Kathmandu 44600, Nepal; paudelmanila@gmail.com (M.P.);

<sup>3</sup> Nepal Health Research Council, Ministry of Health and Population, Ramshah path, Kathmandu 44600, Nepal; bishnu.marasini@gmail.com (B.P.M.);

<sup>4</sup> Bioinformatics and Cheminformatics Division, Scientific Research and Training Nepal P. Ltd., Bhaktapur 44800, Nepal; subinadhikari2018@gmail.com (J.A.S.);

\* Correspondence: swagatstha@gmail.com (R.L.S.S.); subinadhikari2018@gmail.com (J.A.S.);

Scopus Author ID 55969175200

Received: 13.08.2024; Accepted: 6.10.2024; Published: 10.12.2024

**Abstract:** Medicinal plants have been a rich source of bioactive compounds used in treating various diseases since ancient times. Diabetes, a long-term metabolic condition, is affecting a large portion of the global population. Hyperglycemia, which leads to diabetes mellitus, can be managed by inhibiting the human pancreatic  $\alpha$ -amylase enzyme. This study aims to identify potential  $\alpha$ -amylase inhibitors from *Piper longum* L. using different computational methods. From the molecular docking calculations, piperadione, coumapherine, and cepharanone B exhibited good binding affinities of -8.8 kcal/mol, -8.6 kcal/mol, and -8.3 kcal/mol, respectively, better than that of the reference drugs. All the adducts showed significant geometrical stability with smooth RMSD curves from 150 ns molecular dynamics simulations. The thermodynamic stability evaluated through the MMPBSA method in terms of binding free energy changes demonstrated consistent feasibility and spontaneity of the reactions. The hit candidates could be proposed for diabetes management after verification through *in vitro* and *in vivo* experiments.

**Keywords:** diabetes; docking scores; protein-ligand complex; molecular dynamics simulations; Gibbs free energy.

© 2024 by the authors. This article is an open-access article distributed under the terms and conditions of the Creative Commons Attribution (CC BY) license (<https://creativecommons.org/licenses/by/4.0/>).

## 1. Introduction

The use of herbal remedies for treating various illnesses dates back to ancient times and continues in contemporary approaches [1]. Medicinal plants are a rich source of bioactive compounds that can be utilized to treat and manage numerous diseases. Plants produce a variety of secondary metabolites, and their therapeutic properties are the reason for their disease-curing ability [2]. According to the World Health Organization, medicinal plants are an excellent

source of a wide range of medications, with 80% of the developing world still relying on them [3].

*Piper longum* L. (*P. longum*), commonly referred to as long pepper, is a flowering, climbing plant belonging to the Piperaceae family [4]. It is an aromatic plant and is characterized by dioecious traits, trailing growth, and perennial woody roots with jointed stems, thriving in warm environments [5]. *P. longum* has gained significant attention as it is recognized for its potential therapeutic properties against diabetes, depression, cancer, and inflammation [6,7].

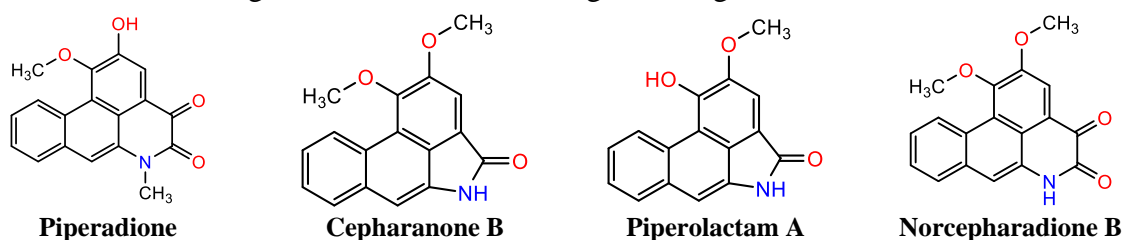
Diabetes mellitus is a chronic metabolic disorder characterized by elevated blood sugar levels resulting from inadequate insulin production or insulin resistance in cells [8]. As per the IDF Diabetes Atlas (2021), approximately 540 million individuals worldwide are currently affected by diabetes, and this figure is projected to rise by 46% by the year 2045 [9]. It has become a leading cause of death globally, claiming approximately 1.5 million lives each year, predominantly in low and middle-income nations [10]. The consumption of starch and its absorption causes a significant increase in postprandial blood glucose levels, and this process is facilitated by the enzyme  $\alpha$ -amylase, which catalyzes the breakdown of  $\alpha$ -(1,4)-D-glycosidic bonds found in starch, converting it into smaller glucose fragments [8]. The inhibition of  $\alpha$ -amylase can manage type II diabetes, and drugs such as voglibose, miglitol, and acarbose are considered effective  $\alpha$ -amylase inhibitors. However, they have numerous side effects like diarrhea, abdominal pain, flatulence, and bloating [11]. These side effects have prompted further research on identifying other potential  $\alpha$ -amylase inhibitors from natural sources with lower or no adverse effects.

The advancement of computational methods has reduced the expenses and time required for experimental procedures to determine complex structures possessing bioactive properties [12]. These methods aim to predict the likely binding modes and affinities between receptors and ligands [13]. Utilizing protein structures, molecular docking evaluates and tests numerous potential binding orientations at the catalytic sites. This research employs a combination of molecular docking, binding free energy calculations, and molecular dynamics simulations (MDS) to identify spatially and thermodynamically the most stable complex and the ligand that could inhibit the receptor protein. This computational study aims to find potential inhibitors of  $\alpha$ -amylase among selected compounds that were isolated from *Piper longum* L. for diabetes management.

## 2. Materials and Methods

### 2.1. Ligands selection and preparation.

The ligands were selected from the literature review of isolated compounds of *P. longum* [14–17] (Figure 1). Their 3D structures were obtained in SDF format from the PubChem database (<https://pubchem.ncbi.nlm.nih.gov/>) [18]. The bond order and molecular structure of selected ligands were examined using the Avogadro software [19].



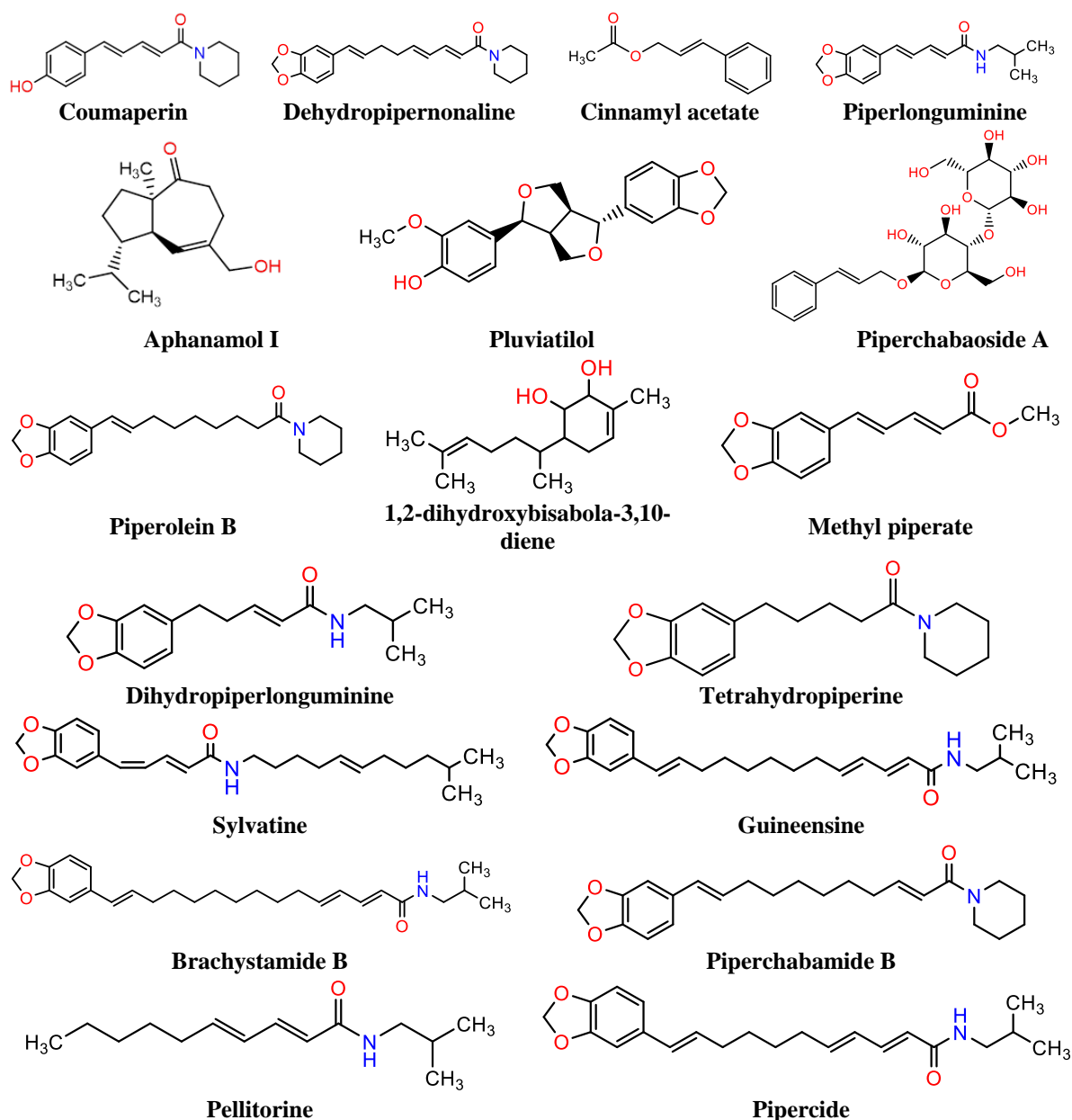


**Figure 1.** Chemical structures of the compounds of *Piper longum*.

### 2.2. Protein preparation.

The high-resolution 3D crystal structure of the human pancreatic  $\alpha$ -amylase enzyme with PDB ID: 2QV4 (X-ray resolution= 1.97 Å, expression system: *Komagataella pastoris*) (<https://doi.org/10.2210/pdb2QV4/pdb>) was retrieved from the RCSB protein data bank server (<https://www.rcsb.org/>) [20]. The protein was visualized using the PyMOL program, cleaned, polar hydrogen was added, and saved in PDB format [21]. The AutoDock Tools was then employed to incorporate polar hydrogen atoms and Kollman charges into the protein structure, after which it was converted to the PDBQT format necessary for molecular docking calculations [22].

### 2.3. Molecular docking calculations.

Molecular docking studies are used to investigate the binding modes between the receptor and ligands and estimate the binding affinity [23]. The AutoDock Vina software was used for molecular docking, where the ligands were allowed to be flexible while keeping the

protein rigid. Parameters such as 20 number of modes, energy range of 4 units, and 32 exhaustiveness were selected for the docking process. The grid center of (14.761, 50.038, 20,977) and the box size of  $46 \times 44 \times 46 \text{ \AA}^3$  with  $0.375 \text{ \AA}$  spacing were employed. The protein-ligand adduct with the highest binding affinity (kcal/mol) was identified, and their 2D and 3D interactions were visualized using the Biovia Discovery Studio program [24]. The docking protocol was validated by obtaining a good RMSD of  $1.30 \text{ \AA}$  through the superimposition of the native ligand from the crystalline complex with the re-docked ligand in the docked complex, as illustrated in Figure 2.

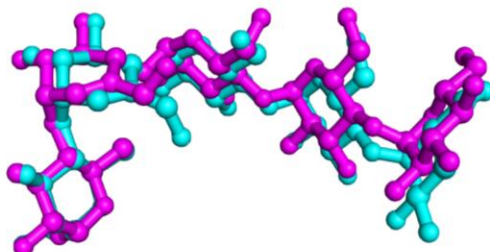


**Figure 2.** Superimposition of the pose of native ligand in the crystal structure (cyan) with the pose of the same ligand obtained from molecular docking calculations (magenta); Heavyatom RMSD=  $1.3 \text{ \AA}$ .

#### 2.4. Molecular dynamics simulation (MDS).

MDS of the top protein-ligand complexes were performed using the GROMACS software (version 2021.2) [25] and Charmm27 force field parameters from the SwissParam server (<https://www.swissparam.ch/>) [26]. TIP3P water model was used to solvate the adducts in a triclinic box system of  $10 \text{ \AA}$  spacing at the sides, and the system was neutralized with counter ions.  $0.15 \text{ M}$  isotonic NaCl solution was added to the system. The equilibration process was carried out at  $310 \text{ K}$  in four stages: two NVT equilibriums followed by two NPT equilibriums, each lasting for  $500 \text{ ps}$ . Additional parameters were taken from recent literature [23], and the final production run for  $150 \text{ ns}$  with  $2 \text{ fs}$  step size was carried out.

#### 2.5. Binding free energy calculation ( $\Delta G_{\text{BFE}}$ ).

The binding free energy change ( $\Delta G_{\text{BFE}}$ ) of the complex was calculated using the MMPBSA method (Poisson Boltzmann solvation model) [27]. The feasibility and spontaneity of the forward reaction were assessed through the free energy changes where an equilibrated portion ( $20 \text{ ns}$ ) of the MD trajectory was used.

The end-state binding free energy change of the complex is given by the equation:

$$\Delta G_{\text{BFE}} = \Delta G_{\text{complex}} - \Delta G_{\text{protein}} - \Delta G_{\text{ligand}} \quad (1)$$

Where  $\Delta G_{\text{ligand}}$ = free energy of ligand,  $\Delta G_{\text{complex}}$ = free energy of protein-ligand complex, and  $\Delta G_{\text{protein}}$ = free energy of protein

### 3. Results and Discussion

#### 3.1. Docking scores.

The docking scores in terms of binding affinity were assessed through molecular docking calculations, which resulted in determining the best binding pose of ligands at the protein's active site [13]. Molecular docking calculation revealed that most of the ligands exhibited better binding affinity compared to that of the reference drugs, as shown in Table 1. However, none of the docked compounds displayed a binding affinity better than that of the

native ligand (-10.4 kcal/mol). Piperadione, coumaperine, and cepharanone B stood out as the top ligands with higher binding affinities, signifying a stronger interaction and binding with the alpha-amylase receptor. The best docking score was obtained, with piperadione having a binding affinity of -8.8 kcal/mol. Coumaperine and cepharanone B demonstrated the binding affinities of -8.6 kcal/mol and -8.3 kcal/mol, respectively.

Similarly, the binding affinities of -8.2 kcal/mol and -8.1 kcal/mol were observed with pluviatilol and piperolactum A, respectively. These values suggested that the ligands were docked at the protein's active site and significant interactions with the amino acid residues were present. Therefore, the compounds from *Piper longum* could potentially inhibit the normal functioning of  $\alpha$ -amylase.

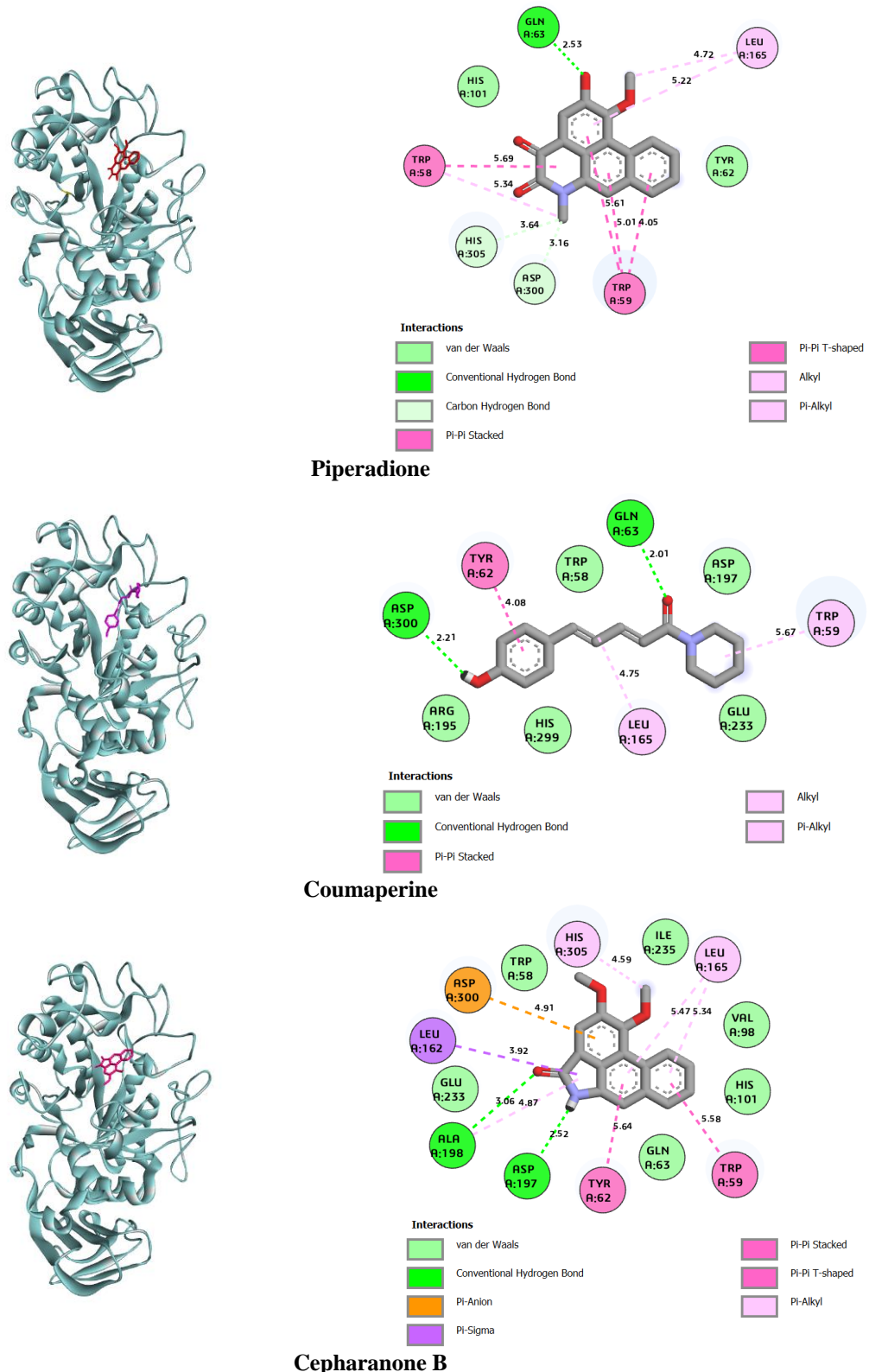
**Table 1.** Binding affinities of ligands of *Piper longum* with human pancreatic  $\alpha$ -amylase (PDB ID: 2QV4).

Ligands	PubChem CID	Binding affinity (kcal/mol)
Piperadione	184116	-8.8
Coumaperine	10131321	-8.6
Cepharanone B	162739	-8.3
Pluviatilol	70695727	-8.2
Piperolactam A	3081016	-8.1
Dehydropiperonaline	6439947	-8.0
Norcepharadione B	189168	-8.0
Piperchabaoside A	44521560	-7.9
Piperlonguminine	5320621	-7.5
Piperolein B	21580213	-7.4
Aphanamol I	11031884	-7.4
1,2-dihydroxybisabola-3,10-diene	52951624	-7.3
Dihydropiperlonguminine	12682184	-7.2
Tetrahydropiperine	581676	-7.2
Sylvatine	131750975	-7.2
Guineensine	6442405	-7.1
Brachystamide B	10047263	-7.1
Methyl piperate	9921021	-7.1
Piperchabamide B	44453655	-7.0
Pipercide	5372162	-7.0
Cinnamyl acetate	5282110	-6.2
Pellitorine	5318516	-6.0
Native	24755467	-10.4
Acarbose	41774	-7.6
Voglibose	444020	-6.1
Miglitol	441314	-5.8

### 3.2. Protein-ligand interactions.

The 2D and 3D representations of the best three complexes with interactions are shown in Figure 3, and the top three ligands occupied the same catalytic site. Both hydrophilic and hydrophobic interactions like Hydrogen bonds, Pi-Alkyl, Alkyl, Pi-Sigma, Pi-Pi T-shaped, Pi-Anion, van der Waals, and Pi-Pi Stacked were observed between the amino acid residues of the protein and ligands as depicted in Table 2. The amino acid residue GLN63 interacted with piperadione and coumaperine, forming strong hydrogen bonds, whereas hydrogen bonds with cepharanone B were observed with ASP197 and ALA198. A carbon-hydrogen bond was formed between piperadione and amino acid residues ASP300 and HIS305. The alkyl interaction was observed with amino acid residue LEU165 with ligands piperadione and coumaperine.

Similarly, the hydrophobic interaction and Pi-interactions were seen between the amino acid TRP59 and all the ligands. ASP300 exhibited Pi-Anion interaction with cepharanone B. Coumapherine and cepharanone B interacted with the catalytic triad: ASP197, GLU233, and ASP300, whereas piperadione interacted with ASP300, forming a hydrogen bond. Several van der Waals interactions were observed between the amino acid residues and ligands.

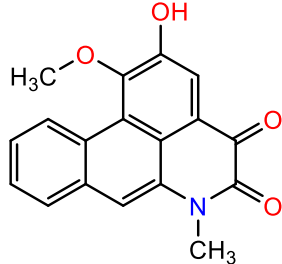
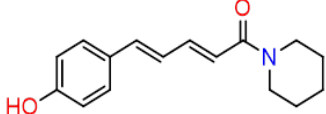
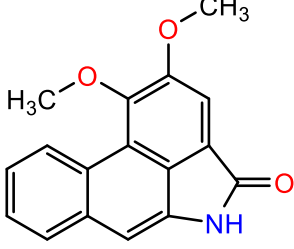


**Figure 3.** 3D representation of the docked ligand at the binding site (left) and 2D interaction (right) of the top three ligands with  $\alpha$ -amylase (PDB ID: 2QV4).



The interactions of the top three ligands with the amino acid residues showed different favorable hydrophilic and hydrophobic interactions and could potentially inhibit the normal functioning of  $\alpha$ -amylase.

**Table 2.** Types of interaction between the top three ligands and amino acid residues of  $\alpha$ -amylase along with distance.

Ligands	Structures	Type of interactions	Active site residues (Distance Å)
Piperadione		Conventional hydrogen bond	GLN63 (2.53)
		Carbon hydrogen bond	ASP300 (3.16), HIS305 (3.64)
		Alkyl	LEU165 (4.72)
		Pi-Alkyl	TRP58 (5.34), LEU165 (5.22), HIS305 (4.34)
		Pi-Pi Stacked	TRP58 (5.69), TRP59 (4.05)
		Pi-Pi T-shaped	TRP59 (5.01, 5.61)
		van der Waals	TYR62, HIS101
Coumaperine		Conventional hydrogen bond	GLN63 (2.01), ASP300 (2.21)
		Alkyl	LEU165 (4.75)
		Pi-Alkyl	TRP59 (5.67)
		Pi-Pi Stacked	TYR62 (4.08)
		van der Waals	TRP58, ARG195, ASP197, GLU233, HIS299
Cepharanone B		Conventional hydrogen bond	ASP197 (2.52), ALA198 (3.06)
		Pi-Sigma	LEU162 (3.92)
		Pi-Alkyl	LEU165 (5.34, 5.47), HIS305 (4.59)
		Pi-Pi Stacked	TYR62 (5.64)
		Pi-Pi T-shaped	TRP59 (5.58)
		Pi-Anion	ASP300 (4.91)
van der Waals	TRP58, GLN63, VAL98, HIS101, GLU233, ILE235		

### 3.3. Stability during production run.

The stability of the protein-ligand adducts is assessed through the root mean square deviation (RMSD) profile retrieved from the MDS trajectory and is shown in Figure 4 [28]. The greater stability of the protein-ligand system is indicated by the lower RMSD of ligands and the smooth nature of curves. All three compounds showed good stability with  $\alpha$ -amylase with acceptable ligand RMSD values. Coumaperine demonstrated greater stability among ligands with an RMSD < 4 Å. Similarly, piperadione and cepharanone B also showed good stability with an RMSD of around 8 Å throughout the simulation run. Despite some spikes in the trajectory, all the ligands attained equilibrium in the last 20 ns of the MDS period.

The protein backbone displayed an exceptionally smooth curve with an RMSD below 2.0 Å, indicating the stability of the protein structure upon ligand binding. No notable structural changes were observed, and the spatial study of the system was hinted at.

The root mean square fluctuation (RMSF) measures the degree of variation and flexibility of protein's amino acid residues over a 150 ns production run. Elevated RMSF values suggest increased flexibility during the simulation, whereas lower values indicate limited changes, signifying a tightly bound protein-ligand complex and improved system stability [29].

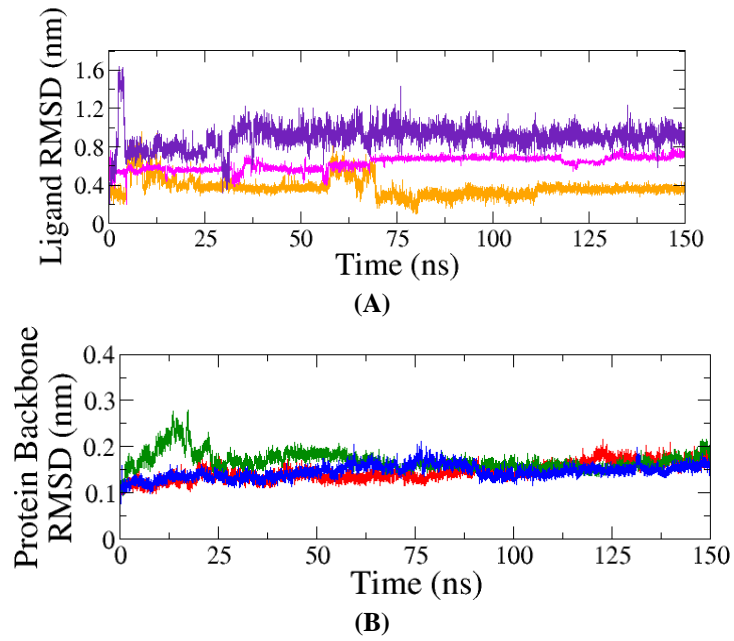


**Figure 4.** (A) RMSD profile of ligands, Coumaperine (orange), Piperadione (magenta), and Cepharanone B (indigo) with respect to protein backbone; (B) RMSD profile of protein backbones with respect to protein backbone in the complexes of Coumaperine (blue), Piperadione (green), and Cepharanone B (red) with the receptor protein.

Similar RMSF plots were obtained for all the studied complexes, as depicted in Figure 5(A). The fluctuation of  $\alpha$ -carbon atoms was below 4.0 Å for all amino acid residues, with an exception at approximately 350 amino acid residue numbers.

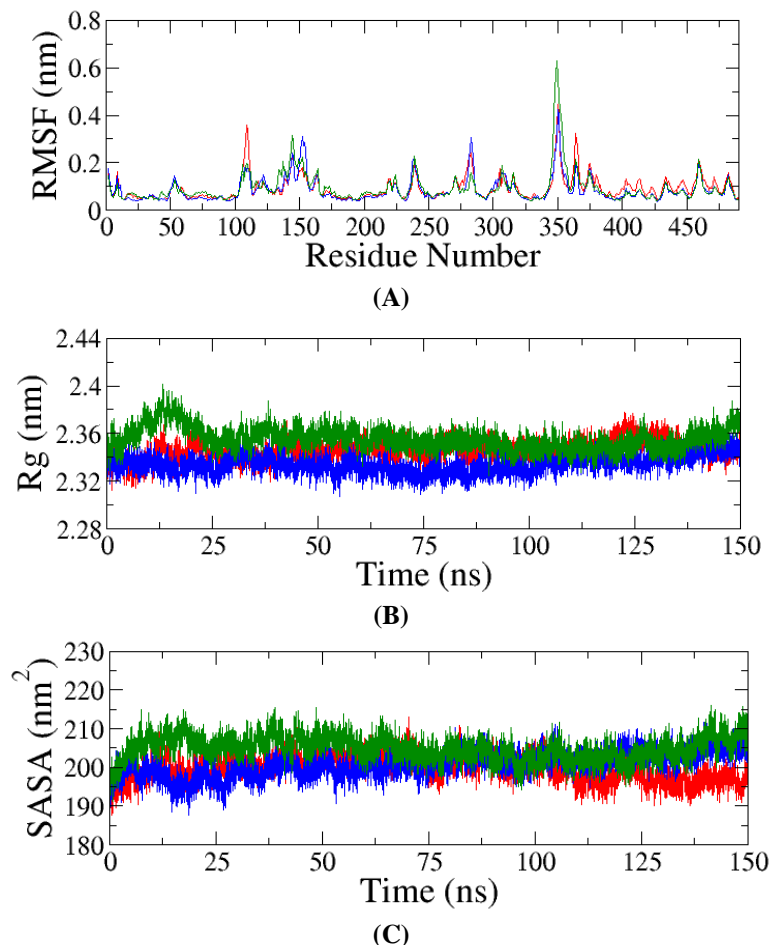


**Figure 5.** (A) RMSF; (B) Rg; (C) SASA of protein in Coumaperine (blue), Piperadione (green), and Cepharanone B (red) protein complexes during MDS.



The radius of gyration ( $R_g$ ) determined from MD simulation indicates the compactness of protein-ligand adducts, with smaller  $R_g$  values signifying a more compact structure [30]. The  $R_g$  calculation showed a stable and smooth trajectory around 23.6 Å, suggesting the stability of all three complexes, as shown in Figure 5(B). The solvent-accessible surface area (SASA) of protein in all three complexes was *ca.* 202±8 nm<sup>2</sup>, as depicted in Figure 5(C). The SASA remained stable throughout the production run, with no significant conformational surface change, indicating no variation in the protein's wettable area upon ligand binding [31]. The SASA, RMSF, and  $R_g$  collectively indicated the geometrical stability of the protein structure with time.

The stability of the adducts is also influenced by the number of conventional hydrogen bonds formed between the ligands and protein molecules, as depicted in Figure 6. An increase in the number of hydrogen bonds typically enhances the stability of the complex [32]. Coumaperine formed a higher number of hydrogen bonds with the receptor compared to piperadione and cepharanone B. This difference in hydrogen bond formation likely contributed to the higher RMSD of piperadione and cepharanone B and the lower RMSD of coumaperine, as shown in Figure 4.

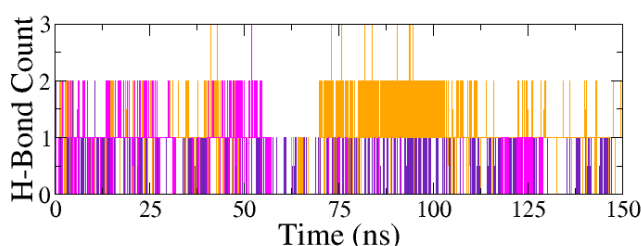


**Figure 6.** Number of hydrogen bond formations between the amino acid residues and Coumaperine (orange), Piperadione (magenta), and Cepharanone B (indigo) during MDS.

Therefore, the comprehensive geometrical evaluation involving RMSD, SASA,  $R_g$ , RMSF, and hydrogen bond count indicated the stability of all three complexes within the catalytic pocket throughout the simulation run. This stability suggests their potential to inhibit the normal functioning of human pancreatic  $\alpha$ -amylase.

### 3.4. Binding free energy changes ( $\Delta G_{BFE}$ ).

The feasibility and spontaneity of complex formation are assessed through the change in binding free energy, as shown in Table 3 and Figure 7. A smaller value of binding free energy change ( $\Delta G_{BFE}$ ) corresponds to higher complex stability [33–35]. When  $\Delta G_{BFE}$  is less than zero ( $\Delta G_{BFE} < 0$ ), it signifies the spontaneity of the complex formation reaction. The values suggested the thermodynamic stability of the complexes, with  $-18.30 \pm 2.48$  kcal/mol for piperadione-amylase,  $-16.12 \pm 3.13$  kcal/mol for coumaperine-amylase, and  $-18.98 \pm 2.02$  kcal/mol for cepharanone B-amylase complexes, respectively. The negative values of  $\Delta G_{BFE}$  for all three complexes indicated the spontaneous nature of the complex formation reaction. Therefore, the compounds piperadione, coumaperine, and cepharanone might be potential inhibitors of human pancreatic  $\alpha$ -amylase.

**Table 3.** Binding free energy change ( $\Delta G_{BFE}$ ) and its components in different complexes.

Complexes	$\Delta E_{VDWAALS}$	$\Delta E_{EEL}$	$\Delta E_{EPB}$	$\Delta E_{NPOLAR}$	$\Delta G_{GAS}$	$\Delta G_{SOLV}$	$\Delta G_{BFE}$
Piperadione	$-29.94 \pm 2.32$	$-11.82 \pm 2.21$	$26.24 \pm 3.05$	$-2.79 \pm 0.18$	$-41.76 \pm 3.28$	$23.46 \pm 2.95$	$-18.30 \pm 2.48$
	$-25.70 \pm 2.90$	$-20.99 \pm 3.95$	$33.89 \pm 4.26$	$-3.33 \pm 0.18$	$-46.68 \pm 4.47$	$30.56 \pm 4.20$	$-16.12 \pm 3.13$
Cepharanone B	$-27.29 \pm 1.74$	$-3.42 \pm 2.31$	$14.32 \pm 2.48$	$-2.59 \pm 0.11$	$-30.71 \pm 3.02$	$11.73 \pm 2.44$	$-18.98 \pm 2.02$

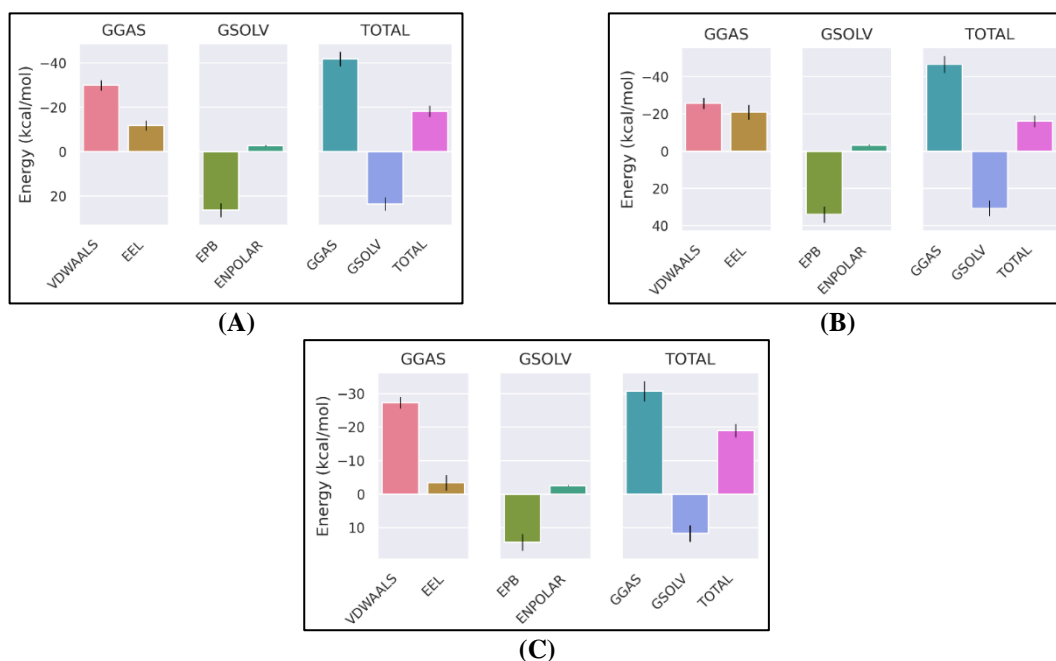


**Figure 7.** Components of binding free energy changes of (A) piperadione; (B) coumaperine; (C) cepharanone B complexes.

#### 4. Conclusions

Among the various phytochemicals of *Piper longum* L., piperadione, coumaperine, and cepharanone B showed the highest binding affinity against  $\alpha$ -amylase through molecular docking. The phytochemicals demonstrated good thermodynamical and geometrical stability in complexes with the  $\alpha$ -amylase protein and could inhibit its normal functioning, contributing to the management of hyperglycemia. However, further *in vivo* and *in vitro* experiments are necessary to validate the preliminary *in silico* results. Plant-based compounds could be a potential alternative to control diabetes mellitus.

#### Funding

This research received no external funding.

#### Acknowledgments

The authors thank Kathmandu Valley College, Kathmandu, Nepal, for the computational resources.

#### Conflicts of Interest

The authors declare no conflict of interest.

#### References

1. Holm, L.R.; Doll, J.; Holm, E.; Pancho, J.V.; Herberger, J.P. *World Weeds: Natural Histories and Distribution*; Wiley: **1997**.
2. K Kumar, A.; Singh, S.K.; Singh, V.K.; Kant, C.; Singh, A.K.; Tripathi, V.; Singh, K.; Sharma, V.K.; Singh, J. An Insight into the Molecular Docking Interactions of Plant Secondary Metabolites with Virulent Factors Causing Common Human Diseases. *S. Afr. J. Bot.* **2022**, *149*, 1008-1016, <https://doi.org/10.1016/j.sajb.2021.11.010>.
3. Vaou, N.; Stavropoulou, E.; Voidarou, C.; Tsigalou, C.; Bezirtzoglou, E. Towards Advances in Medicinal

- Plant Antimicrobial Activity: A Review Study on Challenges and Future Perspectives. *Microorganisms* **2021**, *9*, 2041, <https://doi.org/10.3390/microorganisms9102041>.
4. Kumar, S.; Kamboj, J.; Suman; Sharma, S. Overview for Various Aspects of the Health Benefits of *Piper Longum* Linn. Fruit. *J. Acupunct. Meridian Stud.* **2011**, *4*, 134-140, [https://doi.org/10.1016/S2005-2901\(11\)60020-4](https://doi.org/10.1016/S2005-2901(11)60020-4).
  5. Babu, K.N.; Divakaran, M.; Ravindran, P.N.; Peter, K.V. 25 - Long pepper. In Handbook of Herbs and Spices, Peter, K.V., Ed.; Woodhead Publishing: **2006**; pp. 420-437 <https://doi.org/10.1533/9781845691717.3.420>.
  6. Li, D.; Wang, R.; Cheng, X.; Yang, J.; Yang, Y.; Qu, H.; Li, S.; Lin, S.; Wei, D.; Bai, Y.; Zheng, X. Chemical Constituents from the Fruits of *Piper longum* L. and Their Vascular Relaxation Effect on Rat Mesenteric Arteries. *Nat. Prod. Res.* **2022**, *36*, 674-679, <https://doi.org/10.1080/14786419.2020.1797726>.
  7. Shrestha, R.L.S.; Panta, R.; Maharjan, B.; Shrestha, T.; Bharati, S.; Dhital, S.; Neupane, P.; Parajuli, N.; Marasini, B.P.; Adhikari Subin, J. Molecular Docking and ADMET Prediction of Compounds from *Piper longum* L. Detected by GC-MS Analysis in Diabetes Management. *Mor. J. Chem.* **2024**, *12*, 776-798, <https://doi.org/10.48317/IMIST.PRSM/morjchem-v12i2.46845>.
  8. Kaur, N.; Kumar, V.; Nayak, S.K.; Wadhwa, P.; Kaur, P.; Sahu, S.K. Alpha-Amylase as a Molecular Target for the Treatment of Diabetes Mellitus: A Comprehensive Review. *Chem. Biol. Drug Des.* **2021**, *98*, 539-560, <https://doi.org/10.1111/cbdd.13909>.
  9. Federation, I. D. IDF Diabetes Atlas. International Diabetes Federation, **2021**.
  10. Mohamed, G.A.; Omar, A.M.; El-Araby, M.E.; Mass, S.; Ibrahim, S.R.M. Assessments of Alpha-Amylase Inhibitory Potential of Tagetes Flavonoids through *In Vitro*, Molecular Docking, and Molecular Dynamics Simulation Studies. *Int. J. Mol. Sci.* **2023**, *24*, 10195, <https://doi.org/10.3390/ijms241210195>.
  11. Basnet, S.; Ghimire, M.P.; Lamichhane, T.R.; Adhikari, R.; Adhikari, A. Identification of Potential Human Pancreatic  $\alpha$ -Amylase Inhibitors from Natural Products by Molecular Docking, MM/GBSA Calculations, MD Simulations, and ADMET Analysis. *PLOS ONE* **2023**, *18*, e0275765, <https://doi.org/10.1371/journal.pone.0275765>.
  12. Shrestha, R.L.S.; Neupane, P.; Dhital, S.; Parajuli, N.; Maharjan, B.; Shrestha, T.; Bharati, S.; Marasini, B.P.; Adhikari Subin, J. Selected Phytochemicals as Potent Acetylcholinesterase Inhibitors: An *In Silico* Prediction. *J. Serb. Chem. Soc.* **2024**, 65-65, <https://doi.org/10.2298/JSC240405065S>.
  13. Neupane, P.; Dhital, S.; Parajuli, N.; Shrestha, T.; Bharati, S.; Maharjan, B.; Adhikari Subin, J.; Shrestha, R.L.S. Exploration of Anti-Diabetic Potential of *Rubus ellipticus* smith through Molecular Docking, Molecular Dynamics Simulation, and MMPBSA Calculation. *J. Nepal Phys. Soc.* **2023**, *9*, 95-105, <https://doi.org/10.3126/jnphysoc.v9i2.62410>.
  14. Yadav, V.; Krishnan, A.; Vohora, D. A Systematic Review on *Piper longum* L.: Bridging Traditional Knowledge and Pharmacological Evidence for Future Translational Research. *J. Ethnopharmacol.* **2020**, *247*, 112255, <https://doi.org/10.1016/j.jep.2019.112255>.
  15. Guo, Z.; Xu, J.; Xia, J.; Wu, Z.; Lei, J.; Yu, J. Anti-Inflammatory and Antitumor Activity of Various Extracts and Compounds from the Fruits of *Piper longum* L. *J. Pharm. Pharmacol.* **2019**, *71*, 1162-1171, <https://doi.org/10.1111/jphp.13099>.
  16. Carsono, N.; Tumilaar, S.G.; Kurnia, D.; Latipudin, D.; Satari, M.H. A Review of Bioactive Compounds and Antioxidant Activity Properties of *Piper* Species. *Molecules* **2022**, *27*, 6774, <https://doi.org/10.3390/molecules27196774>.
  17. Biswas, P.; Ghorai, M.; Mishra, T.; Gopalakrishnan, A.V.; Roy, D.; Mane, A.B.; Mundhra, A.; Das, N.; Mohture, V.M.; Patil, M.T.; Rahman, M.H.; Jha, N.K.; Batiha, G.E.-S.; Saha, S.C.; Shekhawat, M.S.; Radha; Kumar, M.; Pandey, D.K.; Dey, A. *Piper longum* L.: A Comprehensive Review on Traditional Uses, Phytochemistry, Pharmacology, and Health-Promoting Activities. *Phytother. Res.* **2022**, *36*, 4425-4476, <https://doi.org/10.1002/ptr.7649>.
  18. Kim, S.; Chen, J.; Cheng, T.; Gindulyte, A.; He, J.; He, S.; Li, Q.; Shoemaker, B.A.; Thiessen, P.A.; Yu, B.; Zaslavsky, L.; Zhang, J.; Bolton, E.E. PubChem 2023 Update. *Nucleic Acids Res.* **2023**, *51*, D1373-D1380, <https://doi.org/10.1093/nar/gkac956>.
  19. Hanwell, M.D.; Curtis, D.E.; Lonie, D.C.; Vandermeersch, T.; Zurek, E.; Hutchison, G.R. Avogadro: An Advanced Semantic Chemical Editor, Visualization, and Analysis Platform. *J. Cheminform.* **2012**, *4*, 17, <https://doi.org/10.1186/1758-2946-4-17>.
  20. Berman, H.M.; Westbrook, J.; Feng, Z.; Gilliland, G.; Bhat, T.N.; Weissig, H.; Shindyalov, I.N.; Bourne, P.E. The Protein Data Bank. *Nucleic Acids Res.* **2000**, *28*, 235-242, <https://doi.org/10.1093/nar/28.1.235>.

21. Yuan, S.; Chan, H.C.S.; Hu, Z. Using PyMOL as a Platform for Computational Drug Design. *WIREs Comput. Mol. Sci.* **2017**, *7*, e1298, <https://doi.org/10.1002/wcms.1298>.
22. Trott, O.; Olson, A.J. AutoDock Vina: Improving the Speed and Accuracy of Docking with a New Scoring Function, Efficient Optimization, and Multithreading. *J. Comput. Chem.* **2010**, *31*, 455-461, <https://doi.org/10.1002/jcc.21334>.
23. Neupane, P.; Adhikari Subin, J.; Adhikari, R. Assessment of Iridoids and Their Similar Structures as Antineoplastic Drugs by *In Silico* Approach. *J. Biomol. Struct. Dyn.* **2024**, 1-16, <https://doi.org/10.1080/07391102.2024.2314262>.
24. Baroroh, U.; Biotek, M.; Muscifa, Z.S.; Destiarani, W.; Rohmatullah, F.G.; Yusuf, M. Molecular Interaction Analysis and Visualization of Protein-Ligand Docking Using Biovia Discovery Studio Visualizer. *Indones. J. Comput. Biol.* **2023**, *2*, 22-30, <https://doi.org/10.24198/ijcb.v2i1.46322>.
25. Abraham, M.J.; Murtola, T.; Schulz, R.; Páll, S.; Smith, J.C.; Hess, B.; Lindahl, E. GROMACS: High Performance Molecular Simulations Through Multi-Level Parallelism from Laptops to Supercomputers. *SoftwareX* **2015**, *1-2*, 19-25, <https://doi.org/10.1016/j.softx.2015.06.001>.
26. Zoete, V.; Cuendet, M.A.; Grosdidier, A.; Michielin, O. SwissParam: A Fast Force Field Generation Tool for Small Organic Molecules. *J. Comput. Chem.* **2011**, *32*, 2359-2368, <https://doi.org/10.1002/jcc.21816>.
27. Valdés-Tresanco, M.S.; Valdés-Tresanco, M.E.; Valiente, P.A.; Moreno, E. gmx\_MMPBSA: A New Tool to Perform End-State Free Energy Calculations with GROMACS. *J. Chem. Theory Comput.* **2021**, *17*, 6281-6291, <https://doi.org/10.1021/acs.jctc.1c00645>.
28. Shrestha, R.L.S.; Maharjan, B.; Shrestha, T.; Marasini, B.P.; Adhikari Subin, J. Geometrical and Thermodynamic Stability of Govaniadine Scaffold Adducts with Dopamine Receptor. *Results Chem.* **2024**, *7*, 101363, <https://doi.org/10.1016/j.rechem.2024.101363>.
29. Abdizadeh, R.; Hadizadeh, F.; Abdizadeh, T. *In Silico* Analysis and Identification of Antiviral Coumarin Derivatives Against 3-Chymotrypsin-Like Main Protease of the Novel Coronavirus SARS-CoV-2. *Mol. Divers.* **2022**, *26*, 1053-1076, <https://doi.org/10.1007/s11030-021-10230-6>.
30. Lobanov, M.Y.; Bogatyreva, N.S.; Galzitskaya, O.V. Radius of Gyration as an Indicator of Protein Structure Compactness. *Mol. Biol.* **2008**, *42*, 623-628, <https://doi.org/10.1134/S0026893308040195>.
31. Durham, E.; Dorr, B.; Woetzel, N.; Staritzbichler, R.; Meiler, J. Solvent Accessible Surface Area Approximations for Rapid and Accurate Protein Structure Prediction. *J. Mol. Model.* **2009**, *15*, 1093-1108, <https://doi.org/10.1007/s00894-009-0454-9>.
32. Chikalov, I.; Yao, P.; Moshkov, M.; Latombe, J.C. Learning Probabilistic Models of Hydrogen Bond Stability from Molecular Dynamics Simulation Trajectories. *BMC Bioinformatics* **2011**, *12*, S34, <https://doi.org/10.1186/1471-2105-12-S1-S34>.
33. Shrestha, R.L.S.; Neupane, P.; Dhital, S.; Parajuli, N.; Maharjan, B.; Shrestha, T.; Bharati, S.; Marasini, B.P.; Adhikari Subin, J. Bioactive Molecules Against Malarial Dihydroorotate Dehydrogenase: An *in silico* Approach. *Mor. J. Chem.* **2024**, *12*, 1742-1769, <https://doi.org/10.48317/IMIST.PRSM/morjchem-v12i4.48008>.
34. Cournia, Z.; Allen, B.; Sherman, W. Relative Binding Free Energy Calculations in Drug Discovery: Recent Advances and Practical Considerations. *J. Chem. Inf. Model.* **2017**, *57*, 2911-2937, <https://doi.org/10.1021/acs.jcim.7b00564>.
35. Adhikari Subin, J.; Shrestha, R.L.S. Computational Assessment of the Phytochemicals of *Panax ginseng* ca Meyer Against Dopamine Receptor D1 for Early Huntington's Disease Prophylactics. *Cell Biochem. Biophys.* **2024**, 1-11, <https://doi.org/10.1007/s12013-024-01426-2>.